Computational Materials Science 84 (2014) 365–373

Contents lists available at ScienceDirect

Computational Materials Science

journal homepage: www.elsevier.com/locate/commatsci

First-principles investigation of the structural, mechanical and electronic properties of the NbO-structured 3d, 4d and 5d transition metal nitrides

Z.T.Y. Liu [a], X. Zhou [b], D. Gall [c], S.V. Khare [a,*]

[a] Department of Physics and Astronomy, The University of Toledo, 2801 West Bancroft Street, Toledo, OH 43606, United States
[b] Department of Chemistry and Biochemistry, University of Maryland at College Park, MD 20742, United States
[c] Department of Materials Science and Engineering, Rensselaer Polytechnic Institute, 110 8th Street, Troy, NY 12180, United States

ARTICLE INFO

Article history:
Received 18 November 2013
Accepted 17 December 2013

Keywords:
Ab initio calculations
Nitrides
Transition metal
Elastic moduli
Hardness
Mechanical properties

ABSTRACT

We have performed *ab initio* calculations on 29 nitride phases of transition metals from the 3d, 4d and 5d rows, in NbO structure. We calculated cohesive energy, lattice constant and elastic constants C_{11}, C_{12} and C_{44}, and derived mechanical moduli, related ratios and hardness. For five out of the ten 3d transition metal nitrides, namely, CrN, MnN, FeN, CoN and NiN, cohesive energy in this new structure is similar to that of the same composition in the rocksalt structure. The lattice constant and bulk modulus were found to be anti-correlated. We observed the correlation between the shear modulus (G), Pugh's ratio (k) and derived Vickers hardness (H_V). For identical metal element significant variations in the mechanical properties of nitrides are found between rocksalt and NbO structures. However for a fixed structure, 3d, 4d and 5d metal nitrides behave similarly. We computed Debye temperature and demonstrated its correlation with H_V as proposed by Madelung, Einstein and Deus. The nitrides, CrN, MoN and WN in NbO structure show values of H_V larger than 20 GPa. We showed systematically that C_{44}, G, k and H_V are anti-correlated with the number of electronic states around E_F, leading to a semi-quantitative link of nitride electronic structure to mechanical instability and hardness. The local density of states demonstrating systematic evolution of the electronic structure with the number of d electrons in the metal atoms was studied. Bader charge transfer from metal to nitrogen atom was analyzed throughout the 29 nitrides showing comparison with rocksalt structure and experimental electronegativity data.

1. Introduction

There has been a large body of work on transition metal nitrides (TMNs) in the search for superhard materials [1–14]. It has been realized that the addition of nitrogen atoms into the high-density electronic gas of transition metals along with the covalent bonding with nitrogen leads to extraordinary hardness [15–18]. Among these compounds, some promising candidates have been experimentally synthesized and studied. These include nitrides of Sc [19–27], Y [21], Ti [28–32], Zr [7,33,34], Hf [7,33,35], V [32,36], Nb [7], Ta [37–42], Cr [39,43–46], Mo [32,39,44,47–49], W [38,44,50], Re [51,52], Fe [53], Os [54,55], Ir [54,56,57], Pd [57,58], Pt [56,59], Cu [60], Au [61–64] and Zn [65].

Apart from experimental studies, density functional theory (DFT) based *ab initio* calculations have helped predict stability, hardness and trends of nitrides with transition metal elements in a large region of the periodic table. Such computations mitigate the high cost of synthesizing and characterizing the materials that do not have promising properties, and eliminate effort on those that cannot exist due to mechanical instability [59,66]. There are systematic computational studies of the transition metal region in the periodic table and different structures in which TMNs crystallize. They include several studies such as one on 3d transition metal nitrides in zincblende, rocksalt and CsCl structures [67], a study on rocksalt-, NiAs- and WC-structured 4d TMNs by Zhao et al. [68], along with another study on more structures of 5d TMNs [69], a study on 5d TMNs in zincblende, rocksalt, fluorite and pyrite structures by Patil et al. [70], and the study of both 4d and 5d TMNs in zincblende and rocksalt structures by Chen and Jiang [71], emphasizing varying aspects of nitride properties such as elastic moduli, mechanical stability, hardness and electronic structure.

Wang et al. proposed a crystal structure (space group $Pm\bar{3}m$), in which TMNs had not been theoretically investigated earlier [72]. Their proposed structure is one obtained by replacing O with N in niobium monoxide (NbO). In their study of four compositions, TcN, ReN, OsN and IrN, the NbO-structured TcN and ReN are more energetically preferred among the other studied cubic, hexagonal and orthorhombic structures with the same composition. The energetic stability of this particular structure over many of these competing ones has motivated the current work. We have systematically explored the properties of NbO-structured TMNs

* Corresponding author. Tel.: +1 419 530 2292.
E-mail address: sanjay.khare@utoledo.edu (S.V. Khare).

0927-0256/$ - see front matter © 2013 Elsevier B.V. All rights reserved.
http://dx.doi.org/10.1016/j.commatsci.2013.12.038

with transition metals in the 3d, 4d and 5d rows. We have also conducted comparisons of the properties of 3d row TMNs in rocksalt (rs) versus NbO structure, because (a) several TMNs have already been synthesized in the rs form, (b) the NbO structure can be viewed as removing one cation and anion pair from the rs cubic cell, (c) the NbO structure has similar values of cohesive energy as rs structure for a number of compositions, which will be shown below and (d) rs- versus NbO-structured nitrides of the same transition metal show large difference in mechanical properties such as hardness, which is also shown in the results section.

Fig. 1 shows the structure of NbO. In a unit cell there are 3 cations and 3 anions, in contrast to 4 cations and 4 anions in that of a rs-structured crystal. The coordination number for both ions is 4 for NbO structure with all the coordinating ions in the same plane. In the rs structure the coordination number is 6 with coordinating ions forming an octahedron. The similar structure but lower coordination number of ions leads to a smaller lattice constant of NbO structure compared to that of the rs structure of the same composition, which is clearly observed in the results that follow. Another view showing the cubic symmetry is provided in Ref. [72].

2. Computational method

We performed first-principles total energy calculations with density functional theory (DFT) [73]. The suit of codes, Vienna *Ab initio* Simulation Package (VASP) [74–76] was used with Ultra-soft Vanderbilt pseudo-potentials (US-PP) [77] as supplied by Kresse and Hafner [78], within the local density approximation (LDA) [79] and PW91 general gradient approximation (GGA) [80]. LDA is known to underestimate the lattice constant and overestimate the cohesive energy and elastic constants, while GGA does the opposite for lattice constants and elastic constants by a smaller upper bound and provides more precise cohesive energy values [81,82]. Hence, we did calculations of the lattice constant, elastic constants and cohesive energy with both of those two approximations, and the derivation of mechanical properties with effective medium theory using only GGA data. We chose the kinetic energy cutoff value to the plane-wave basis set of the single-particle wave function expansion to be 450 eV for all compounds, and high precision mode in VASP. The electronic self-consistent loops were set to converge below 10^{-4} eV/atom. For k-points we used a $12 \times 12 \times 12$ Monkhorst–Pack mesh [83,84]. Tests using a higher energy cutoff value and denser k-point mesh suggested that total energy convergence below ±1 meV was reached.

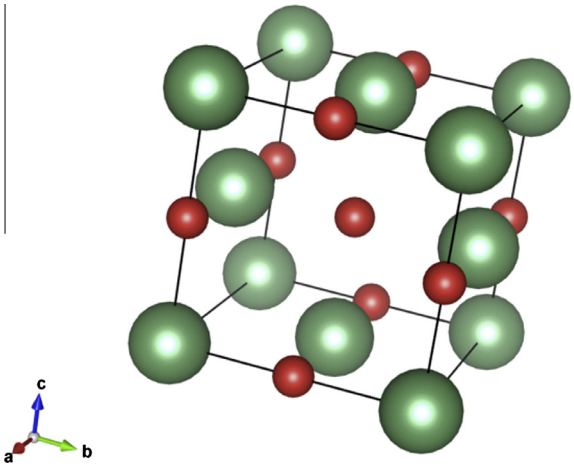

Fig. 1. The structure of NbO. The large green balls depict niobium cations at [0,0,0], [½,½,0], [½,0,½], and small red ones represent oxygen anions at [0,½,0], [0,0,½], [½,½,½]. In an alternative view of the same structure, the cations and anions may be interchanged.

Lattice constants (a) were varied in a range of 1 Å surrounding the minimum energy configuration. This data was fit to the Murnaghan equation of state [85,86] to get an initial estimate of the equilibrium lattice constant (a_M). Further refinement was then performed by varying lattice constants, over a range of $a_M \pm 0.03$ Å, in steps of 0.01 Å. These refined results were fit to a second order polynomial to obtain the final equilibrium value. Bulk modulus was also calculated in this step as a consistency check to be compared with the one calculated from the elastic constants later.

From the output of VASP computational run at the equilibrium lattice constant we achieved total energy per formula unit of each phase in equilibrium (E_{MN}). We also calculated the total energy of the transition metal (E_{M}) and nitrogen (E_{N}) atoms, and define cohesive energy per atom (E_{coh}) as $E_{coh} = (E_{\mathrm{M}} + E_{\mathrm{N}} - E_{\mathrm{MN}})/2$. A large positive value of E_{coh} is indicative of high stability.

For obtaining the three independent single crystal elastic constants for cubic systems, C_{11}, C_{12} and C_{44}, we applied three sets of strains to our primitive cells and fit the resultant total energy to second order polynomials. The polynomial coefficients were used to solve three linear equations to determine the elastic constants, primarily as detailed by Patil et al. [66]. The only difference from their approach was our choice of strains for computing the composite elastic constant (C_{11}–C_{12}). We selected the volume-conserving orthorhombic set of strains, of Mehl et al. [87,88], which is better than the similar volume-conserving tetragonal one due to the absence of third order terms [87]. Ionic relaxation into equilibrium was achieved by the conjugate-gradient algorithm until a force tolerance of 0.01 eV/Å was reached for each atom. The strains were chosen to be below 3% to maintain quadratic behavior of the energy with the varied lattice.

With the three independent elastic constants, we calculated the mechanical properties of the material, including the bulk modulus (B) given by $B = (C_{11} + 2C_{12})/3$, the polycrystalline shear modulus in various forms like Voigt approximation (G_V), Reuss approximation (G_R) and Hill's arithmetic mean (G) as given by:

$$G_V = [(C_{11} - C_{12}) + 3C_{44}]/5, \tag{1}$$

$$G_R = [5(C_{11} - C_{12})C_{44}]/(4C_{44} + 3C_{11} - 3C_{12}), \tag{2}$$

$$G = (G_V + G_R)/2. \tag{3}$$

From these we may further obtain Pugh's ratio (k) as $k = G/B$, Poisson's ratio (υ) as $\upsilon = (3 - 2k)/[2(3 + k)]$, polycrystalline Young's modulus (E) as $E = 9G/(3 + k)$. Using B and G, Chen et al. [17] provided a derivation for Vickers hardness, $H_{VC} = 2(k^2G)^{0.585} - 3$. Tian et al. [18] modified it to always obtain positive values of H_V as:

$$H_{VT} = 0.92k^{1.137}G^{0.708}. \tag{4}$$

We have used this form in our analysis. Values for G and B also yield the Debye temperature (θ_D) which has a more complex form given in Eqs. (5) and (6) below.

$$\theta_D = \frac{h}{k_B}\left[\frac{3n}{4\pi}\left(\frac{N_A\rho}{M}\right)\right]^{1/3} \upsilon_m, \quad \text{where} \quad \upsilon_m = \left[\frac{1}{3}\left(\frac{2}{\upsilon_t^3} + \frac{1}{\upsilon_l^3}\right)\right]^{-1/3}, \tag{5}$$

$$\upsilon_t = \left(\frac{G}{\rho}\right)^{1/2} \quad \text{and} \quad \upsilon_l = \left(\frac{3B + 4G}{3\rho}\right)^{1/2}. \tag{6}$$

Here h is Planck's constant, k_B Boltzmann's constant, N_A Avogadro's number, ρ the mass density, M the molecular weight of the primi-

tive cell and n the number of atoms in the cell for which M is calculated. The transverse, longitudinal and mean sound speeds are v_t and v_l and v_m respectively.

Debye temperature and hardness are two quantities both determined by the nature of bonding between different atoms in a crystal. Therefore we may expect a connection between the two. Abrahams et al. [89] replaced B with H_V in the formula, $\theta_D = a \times B^{1/2}\rho^{-1/6}M^{-1/3}$ first derived by Madelung [90] and Einstein [91,92] because it is easy to measure H_V experimentally. Deus and Schneider [93] then added a constant to the linear formula to get better accuracy. Their formula is expressed as

$$\theta_D = a \times H_V^{1/2}\rho^{-1/6}M^{-1/3} + b, \tag{7}$$

where a and b are linear fitting coefficients in the equation.

The electronic density of states, local or projected (LDOS) and total (TDOS) were computed with GGA potentials, using tetrahedron method with Blöchl corrections [94] for the energy and gamma point centered meshes that are 1.5 times denser than those used for other computations.

The 29 phases we studied have the same structure. Therefore, any trend in the charge transfer from the transition metal atom to nitrogen atom can be easily observed. To investigate whether a trend exists we used Bader charge analysis as developed by Arnaldsson et al. [95–98], implementing Bader's division scheme [99,100], and PAW–GGA potentials, including semi-core electrons when available were used [101]. With the new potentials, we determined the equilibrium lattice constants following the method detailed earlier. Then a $250 \times 250 \times 250$ FFT grid was used to give reliable charge transfer results.

3. Results and discussion

Tables 1–3 show the calculated equilibrium lattice constant (a), elastic constants C_{11}, C_{12}, C_{44}, mechanical stability and E_{coh} of all our compounds with both LDA and GGA. E_{coh} under GGA of all 29 phases was plotted against the group number of the corresponding transition metal in Fig. 2. In addition, the theoretical values under GGA for rs-structured 3d TMNs from Table 1 and experimental values for the same phases from Ref. [102] are also shown. We see good agreement between the calculated and experimental values for these phases. NbO-structured ScN, TiN, VN, CuN and ZnN have cohesive energy values lower than those of their rs-structured counterparts, indicating their lower energetic stability. The other NbO-structured 3d TMNs, namely CrN, MnN, FeN, CoN and NiN, have similar values of cohesive energy as the corresponding rs-structured ones suggesting that they have similar stability. For all of these nitrides, if rs-structured phases can be experimentally synthesized, NbO structure should be another close possibility. Our results should motivate experimental effort towards synthesis of these new NbO-structured phases.

In order to be mechanically stable, a compound of a specific crystallographic system should satisfy a set of criteria. For a structure in the cubic system, such as the NbO structure, it should satisfy

$$C_{11} - C_{12} > 0, \quad C_{11} + 2C_{12} > 0, \quad C_{11} > 0 \quad \text{and} \quad C_{44} > 0. \tag{8}$$

In our study, we found only 3 out of 29 compounds, namely CuN, ZnN and CdN, to be unstable under both LDA and GGA. In addition, AgN was found to be marginally stable under LDA and unstable under GGA. All of them only violate the criterion for C_{44} to be positive. All of this unstable behavior is restricted to the transition metal group number 11 and 12 of 3d and 4d rows.

From the equations listed above we computed B, G, E, k, v, H_{VT} and θ_D from our computed fundamental elastic constants C_{11}, C_{12}, C_{44}. Table 4 lists B, G and E. To better observe trends across the periodic table, the plots of a and B are drawn in Fig. 3. For comparison, the calculated values under GGA for rs-structured nitrides with 3d transition metals from Ref. [67] are also included. Values of the lattice constant show a trough at metal group number 8 (Fe, Ru and Os) and those of B show a peak at metal group number 7 (Mn, Tc and Re). We see the clear anti-correlation between a and B among nitrides with transition metals of the same row. However, for nitrides with the same group of metals but of different rows, there is no clear evidence of anti-correlation. Specifically, the 3d row is generally associated with the smallest values of lattice constant (a) while 4d and 5d rows with similar and larger values. For B the 5d row is associated with the largest values while 3d and 4d rows with similar and smaller values. In addition, the anti-correlation among nitrides with 3d metals in different structures is not observed when we compare values for NbO and rs structures in Fig. 3.

Table 5 shows values of k, v, H_{VT} and θ_D. Fig. 4 displays G, k and H_{VT} to better illustrate the similarity in their trends. The theoretical values under GGA for rs-structured nitrides with 3d transition metals from Ref. [67] are also included for comparison. Pugh's ratio (k) is defined as G/B, and the variation range of B is much smaller than that of G in our study. These two observations imply that G and k have similar trends. Furthermore, H_{VT} from Eq. (4), is the product of positive powers of G and k, so it behaves similar to those two quantities. Within each panel in Fig. 4, the NbO-structured nitrides with transition metals of the 3d, 4d and 5d rows behave similarly, peaking at metal group number 6 (Cr, Mo and W), and then slowly decreasing. If one knows an element associated with high value of hardness, it is possible that elements in the same group are also good candidates in the same structure. Note that the rs-structured nitrides behave differently from the NbO-structured ones. This means nitrides with the same composition but in different structures behave differently and it is difficult to predict the

Table 1
Lattice constant (a), elastic constants (C_{11}, C_{12}, C_{44}), mechanical stability and cohesive energy per atom (E_{coh}) of the NbO-structured 3d transition metal (M) nitrides (MN). Stable phases are denoted as "S" and unstable ones as "U". Values of E_{coh} for rocksalt (rs)-structured phases under GGA are also listed.

M	a (Å)		C_{11} (GPa)		C_{12} (GPa)		C_{44} (GPa)		Mechanical stability		E_{coh} (eV/atom)		
	LDA	GGA	LDA	GGA	LDA	GGA	LDA	GGA	LDA	GGA	LDA	GGA	rs (GGA)
Sc	4.371	4.454	312.2	269.3	67.8	64.1	33.7	37.1	S	S	5.96	5.11	6.50
Ti	4.065	4.136	454.0	383.7	122.0	116.6	52.7	52.5	S	S	7.06	6.00	7.01
V	3.887	3.955	504.1	422.1	202.6	186.9	50.0	37.4	S	S	6.90	5.64	6.08
Cr	3.769	3.836	783.0	666.8	127.7	118.7	150.4	143.5	S	S	6.00	4.57	4.58
Mn	3.709	3.779	743.8	624.0	164.8	149.1	135.1	127.7	S	S	5.71	4.23	4.15
Fe	3.689	3.762	643.4	526.5	200.8	179.6	126.9	114.4	S	S	6.13	4.73	4.64
Co	3.692	3.772	493.2	390.7	239.7	209.3	110.8	98.8	S	S	6.06	4.96	4.97
Ni	3.734	3.822	451.7	352.4	200.5	172.1	52.2	41.3	S	S	5.39	4.25	4.36
Cu	3.858	3.961	304.9	231.0	162.6	135.4	−2.5	−2.7	U	U	4.06	3.04	3.29
Zn	4.015	4.130	248.3	189.1	112.2	90.1	−40.0	−43.3	U	U	2.81	1.94	2.42

Table 2
Lattice constant (a), elastic constants (C_{11}, C_{12}, C_{44}), mechanical stability and cohesive energy per atom (E_{coh}) of the NbO-structured 4d transition metal (M) nitrides (MN). Stable phases are denoted as "S" and unstable ones as "U".

M	a (Å)		C_{11} (GPa)		C_{12} (GPa)		C_{44} (GPa)		Mechanical stability		E_{coh} (eV/atom)	
	LDA	GGA	LDA	GGA	LDA	GGA	LDA	GGA	LDA	GGA	LDA	GGA
Y	4.719	4.807	260.9	226.2	50.1	48.0	25.1	27.9	S	S	5.89	5.14
Zr	4.406	4.475	388.9	340.6	112.1	105.2	42.6	39.7	S	S	7.60	6.52
Nb	4.201	4.263	477.8	411.7	193.3	180.7	50.3	42.1	S	S	7.98	6.68
Mo	4.067	4.125	812.1	715.1	122.1	108.5	139.8	139.3	S	S	7.44	5.97
Tc	3.999	4.061	743.9	628.2	176.0	163.2	136.2	127.0	S	S	7.47	6.03
	3.975[a]	4.032[a]	748[a]	643[a]	181[a]	166[a]	154[a]	140[a]				
Ru	3.981	4.049	629.3	517.9	206.0	185.9	110.5	100.7	S	S	7.03	5.64
Rh	4.005	4.083	468.3	362.5	227.4	201.2	93.8	83.5	S	S	6.13	4.85
Pd	4.073	4.167	370.9	283.0	179.5	147.7	39.3	31.8	S	S	4.39	3.21
Ag	4.243	4.374	231.0	165.0	114.3	86.4	1.5	−1.8	S	U	3.00	1.99
Cd	4.434	4.570	195.0	132.2	75.8	59.2	−5.4	−11.1	U	U	2.23	1.41

[a] Wang et al. [72] (LDA and GGA).

Table 3
Lattice constant (a), elastic constants (C_{11}, C_{12}, C_{44}), mechanical stability and cohesive energy per atom (E_{coh}) of the NbO-structured 5d transition metal (M) nitrides (MN). Stable phases are denoted as "S" and unstable ones as "U".

M	a (Å)		C_{11} (GPa)		C_{12} (GPa)		C_{44} (GPa)		Mechanical stability		E_{coh} (eV/atom)	
	LDA	GGA	LDA	GGA	LDA	GGA	LDA	GGA	LDA	GGA	LDA	GGA
N/A	N/A	N/A	N/A	N/A	N/A	N/A	N/A	N/A	N/A	N/A	N/A	N/A
Hf	4.331	4.407	435.3	373.5	116.2	111.5	58.5	54.3	S	S	7.78	6.77
Ta	4.191	4.236	511.6	439.4	224.2	203.0	54.8	44.0	S	S	8.73	7.53
W	4.063	4.120	903.0	812.8	131.2	115.1	174.3	170.7	S	S	8.63	7.13
Re	4.012	4.070	817.9	704.1	207.1	194.7	155.6	143.4	S	S	7.94	6.46
	4.000[a]	4.061[a]	838[a]	734[a]	205[a]	188[a]	173[a]	160[a]				
Os	4.003	4.064	684.4	573.8	249.8	229.9	113.0	119.5	S	S	7.66	6.24
		4.051[a]		574[a]		238[a]		108[a]				
Ir	4.041	4.111	464.6	363.8	288.0	261.5	88.5	80.0	S	S	6.83	5.47
		4.159[a]		370[a]		263[a]		60[a]				
Pt	4.115	4.197	356.5	265.4	247.8	215.1	27.1	17.5	S	S	5.36	4.09
Au	4.266	4.387	218.1	160.3	159.9	122.4	20.1	15.1	S	S	3.34	2.23
Hg	4.487	4.639	155.1	129.9	92.6	61.2	10.4	4.7	S	S	1.60	0.70

[a] Wang et al. [72] (LDA and GGA).

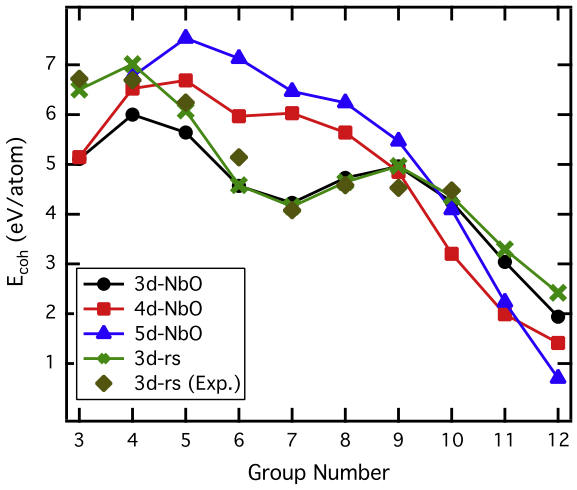

Fig. 2. Cohesive energy per atom of the NbO-structured nitrides (MN) versus the group number of their corresponding transition metals (M). The nitrides corresponding to metals (M) from the 3d, 4d and 5d rows are represented by black circles, red squares and blue triangles respectively. For instance, group number 4 stands for Ti (black circle), Zr (red square) and Hf (blue triangle). For comparison, calculated values for 3d metal, rocksalt (rs)-structured nitrides are represented by green ×, and corresponding experimental values from Ref. [102] are represented by dark yellow ♦. (For interpretation of the references to color in this figure legend, the reader is referred to the web version of this article.)

hardness of one based on that of the other simply because they have the same transition metal. Specifically, (a) rs-CrN has a small value of H_{VT} (1.2 GPa), but value of NbO-structured CrN is 21.6 GPa. (b) rs-MnN and rs-FeN are mechanically unstable in Ref. [67] because of C_{44} being negative, but NbO-structured MnN and NbO-structured FeN are mechanically stable and have high values of H_{VT} (16.7 GPa and 12.2 GPa respectively). Note in Fig. 2 that CrN, MnN and FeN have very similar values of E_{coh} for rs and NbO structures. One might therefore experimentally obtain their NbO-structured phases having high values of hardness when rs-structured phases are of low values of hardness or are mechanically unstable. These observations show that extrapolation of material properties for compounds with the same stoichiometry and crystal symmetry, cubic in this case, is not possible. This is also observed in Ref. [67]. Such variations in properties underscore the importance of the systematic investigation of mechanical properties undertaken in the present work and by others [67–71].

Fig. 5 shows the correlation of our computed θ_D from Eq. (5) with H_{VT} from Eq. (4). The relationship is well represented by the fitting line. It demonstrates that the same set of fitting parameters is applicable to the same structure, regardless of the transition metal involved, thus verifying the relationship denoted by Eq. (7).

Figs. 6 and 7 show the LDOS of 7 nitrides. In Fig. 6, YN, TcN and AgN contain transition metals of the same row. We observe that as the group number of metals increases from 3 (Y) to 7 (Tc) and then to 11 (Ag), the major peaks, associated with the metal M-d orbitals, shift to lower energy and tend to fall below E_F. This is because more electronic states are included below E_F as the number of electrons increases with group number. The minor peaks on the far left, corresponding to the M-s orbitals, shift to lower regions and then to higher regions from E_F. This trend correlates with that found for

Table 4
Bulk modulus (B), polycrystalline shear modulus (G) and Young's modulus (E) of the NbO-structured 3d, 4d and 5d transition metal (M) nitrides (MN). Unstable phases are denoted as "U" without a numerical value.

M			B (GPa)			G (GPa)			E (GPa)		
Sc	Y	N/A	132.5	107.4	N/A	56.5	45.5	N/A	148.5	119.5	N/A
Ti	Zr	Hf	205.6	183.7	198.8	77.1	62.5	78.0	205.7	168.3	206.8
V	Nb	Ta	265.3	257.7	281.8	60.5	64.0	66.3	168.6	177.3	184.3
Cr	Mo	W	301.4	310.7	347.7	186.5	191.4	228.2	463.7	476.3	561.8
Mn	Tc	Re	307.4	318.2	364.5	164.1	162.2	180.8	418.0	415.9	465.5
Fe	Ru	Os	295.2	296.6	344.6	135.2	123.1	138.3	351.9	324.5	366.0
Co	Rh	Ir	269.7	255.0	295.6	95.5	82.3	66.9	256.2	223.0	186.5
Ni	Pd	Pt	232.2	192.8	231.9	56.8	43.3	20.2	157.6	120.8	59.0
Cu	Ag	Au	167.3	112.6	135.0	U	U	16.5	U	U	47.6
Zn	Cd	Hg	123.1	83.6	84.1	U	U	11.9	U	U	34.0

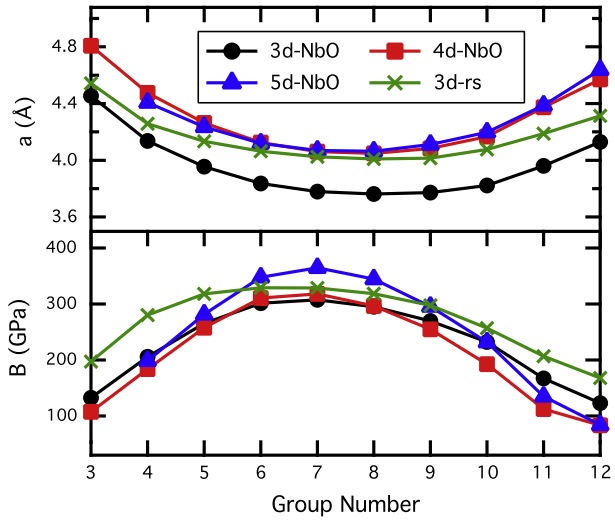

Fig. 3. Computed equilibrium lattice constant (a) and bulk modulus (B) of the NbO-structured nitrides (MN) versus the group number of their corresponding transition metals (M). The nitrides corresponding to metals (M) from the 3d, 4d and 5d rows are represented by black circles, red squares and blue triangles respectively. For instance, group number 5 stands for V (black circle), Nb (red square) and Ta (blue triangle). For comparison, 3d metal, rocksalt (rs)-structured nitrides are represented by green ×. The data in the two panels suggests anti-correlation of B with a. (For interpretation of the references to color in this figure legend, the reader is referred to the web version of this article.)

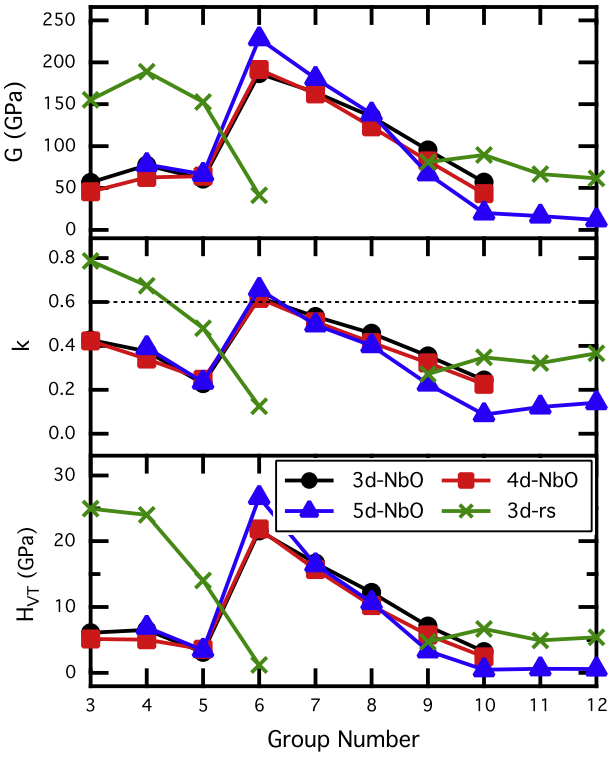

Fig. 4. Polycrystalline shear modulus (G), Pugh's ratio (k) and Vickers Hardness (H_{VT}) from Eq. (4) of the NbO-structured nitrides (MN) versus the group number of their corresponding transition metals (M). The nitrides corresponding to metals (M) from the 3d, 4d and 5d rows are represented by black circles, red squares and blue triangles respectively. For instance, group number 7 stands for Mn (black circle), Tc (red square) and Re (blue triangle). For comparison, 3d metal, rocksalt (rs)-structured nitrides are represented by green ×. For mechanically unstable nitrides, data has not been shown leading to breaks in lines, which are only a guide to the eye. (For interpretation of the references to color in this figure legend, the reader is referred to the web version of this article.)

the peaking of values of B in Fig. 3. In Fig. 7, we observe the LDOS of CrN, MoN and WN, which have transition metals of the same group. These were chosen for comparison since they show the highest G, k and H_{VT} values. We observe that the positions of M-d peaks, with respect to E_F, are very similar. In addition, VN is provided for comparison as an adjacent group transition metal nitride, which has much lower G, k and H_{VT} values. Its peak has a right shift compared with the other three compounds, consistent with the trend in Fig. 6.

Table 5
Pugh's ratio (k), Poisson's ratio (v), Vickers hardness (H_{VT}) and Debye temperature (θ_D) of the NbO-structured 3d, 4d and 5d transition metal (M) nitrides (MN). Unstable phases are denoted as "U" without a numerical value.

M			k			v			H_{VT} (GPa)			θ_D (K)		
Sc	Y	N/A	0.43	0.42	N/A	0.31	0.31	N/A	6.1	5.2	N/A	560.4	395.3	N/A
Ti	Zr	Hf	0.38	0.34	0.39	0.33	0.35	0.33	6.5	5.0	6.9	617.4	444.0	363.0
V	Nb	Ta	0.23	0.25	0.24	0.39	0.39	0.39	3.1	3.6	3.5	526.1	437.4	328.8
Cr	Mo	W	0.62	0.62	0.66	0.24	0.24	0.23	21.6	21.9	26.7	885.2	720.5	585.4
Mn	Tc	Re	0.53	0.51	0.50	0.27	0.28	0.29	16.7	15.7	16.4	809.4	655.3	518.3
Fe	Ru	Os	0.46	0.42	0.40	0.30	0.32	0.32	12.2	10.2	10.7	730.7	564.9	450.5
Co	Rh	Ir	0.35	0.32	0.23	0.34	0.35	0.39	7.1	5.8	3.3	604.9	462.4	316.6
Ni	Pd	Pt	0.24	0.22	0.09	0.39	0.40	0.46	3.2	2.4	0.5	473.3	335.6	176.2
Cu	Ag	Au	U	U	0.12	U	U	0.44	U	U	0.6	U	U	161.7
Zn	Cd	Hg	U	U	0.14	U	U	0.43	U	U	0.6	U	U	139.7

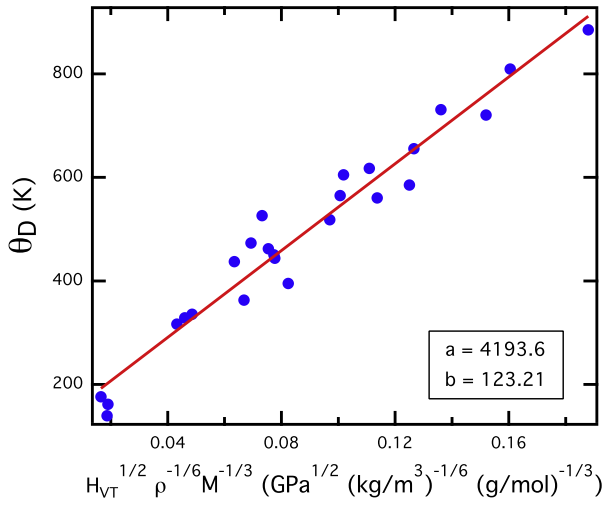

Fig. 5. Computed Debye temperature (θ_D) from Eq. (5) versus Vickers hardness (H_{VT}) from Eq. (4). Symbols are data points that have been shown only for mechanically stable structures. The lines are linear fits to Eq. (7).

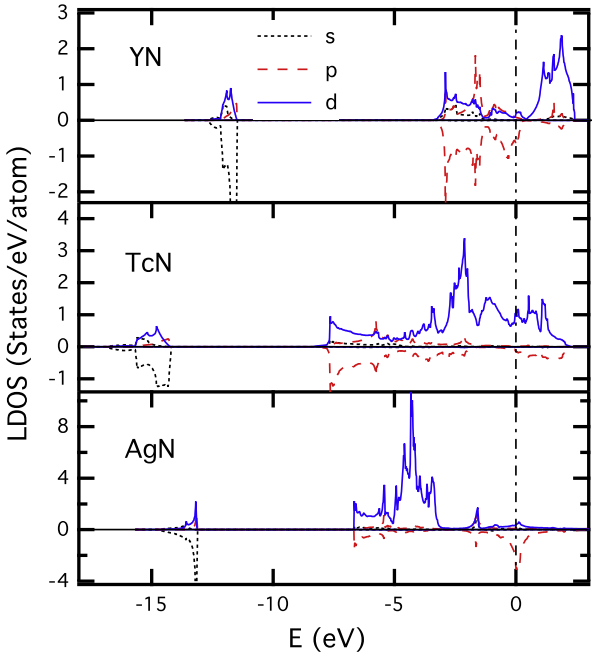

Fig. 6. Local density of states (LDOS) of NbO-structured YN, TcN and AgN. Nitrogen LDOS have been plotted as negative values for clarity. The most prominent peaks depict the hybridization of metal d orbitals with nitrogen p orbitals. Fermi energy is set to zero in each panel.

To better understand the electronic nature of high hardness and mechanical instability, we analyzed the electronic states around E_F. Previous literature has already hinted at a correlation between the total density of electronic states (TDOS) at E_F and instability [70]. Since the changes of peaks are sharp, instead of TDOS, the integral of TDOS around E_F, i.e. the number of electronic states within a window of $E_F \pm 0.2$ eV is used to draw the plot. On the other hand, as hardness is affected greatly by G, which relies upon elastic constant C_{44}, and instability is also associated closely with it, we plotted C_{44} obtained with GGA. In Fig. 8, the trend of C_{44} is similar to those of G, k and H_{VT}. The anti-correlation of C_{44} with the number of electronic states around E_F is obvious for nitrides with 4d and 5d

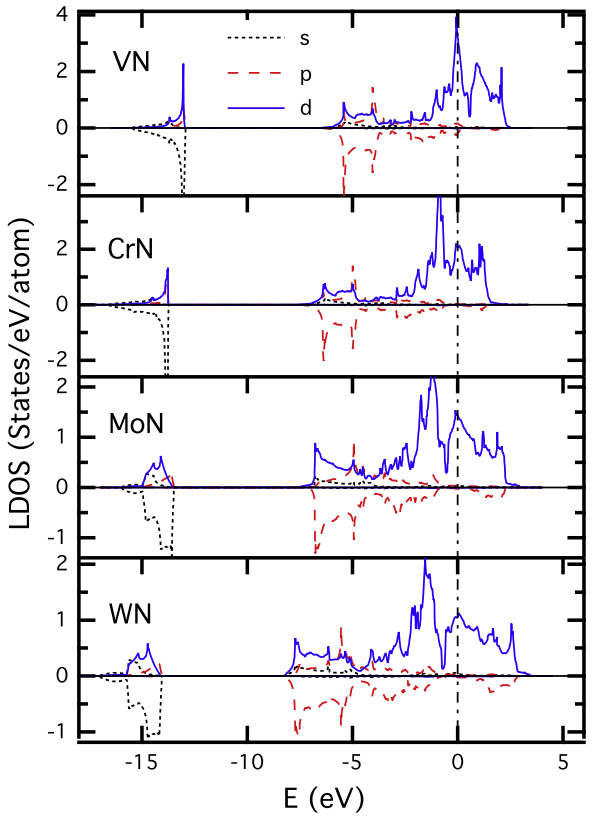

Fig. 7. Local density of states (LDOS) of NbO-structured, group 5 nitride VN and group 6 nitrides CrN, MoN and WN. Nitrogen LDOS have been plotted as negative values for clarity. The most prominent peaks depict the hybridization of metal d orbitals with nitrogen p orbitals. Fermi energy is set to zero in each panel.

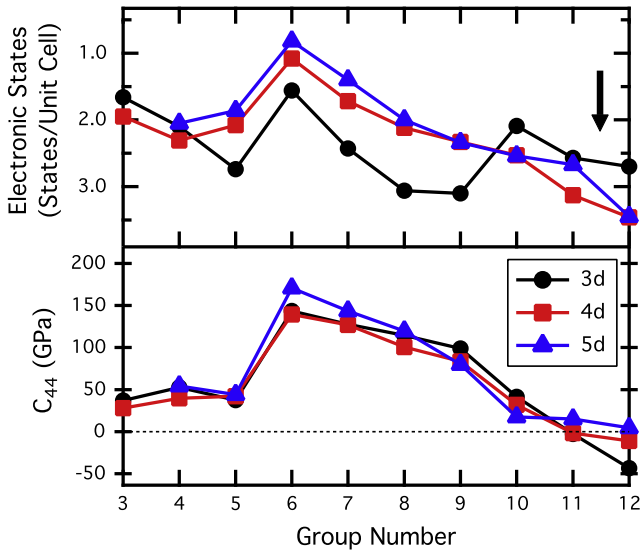

Fig. 8. The number of electronic states per unit cell around E_F (from −0.2 eV to 0.2 eV) and elastic constant C_{44} of the NbO-structured nitrides (MN) versus the group number of their corresponding transition metals (M). The nitrides corresponding to metals (M) from the 3d, 4d and 5d rows are represented by black circles, red squares and blue triangles respectively. For instance, group number 11 stands for Cu (black circle), Ag (red square) and Au (blue triangle). The arrow indicates the inverted y-axis in the top panel. The data in the two panels suggests anti-correlation of C_{44} with the number of electronic states around E_F. (For interpretation of the references to color in this figure legend, the reader is referred to the web version of this article.)

Table 6
Electronegativity (χ) of the metals and Bader charge transfer (q_{trans}) from metal (M) atoms to nitrogen (N) atoms of the 3d, 4d and 5d metal, NbO-structured nitrides (MN) and 3d metal, rocksalt (rs)-structured nitrides (MN).

M			χ			q_{trans} (NbO)			q_{trans} (rs)
Sc	Y	N/A	1.20	1.11	N/A	1.39	1.46	N/A	1.79
Ti	Zr	Hf	1.32	1.22	1.23	1.38	1.50	1.52	1.74
V	Nb	Ta	1.45	1.23	1.33	1.29	1.43	1.49	1.61
Cr	Mo	W	1.56	1.30	1.40	1.14	1.26	1.40	1.44
Mn	Tc	Re	1.60	1.36	1.46	1.05	1.11	1.25	1.33
Fe	Ru	Os	1.64	1.42	1.52	0.93	0.91	1.07	1.20
Co	Rh	Ir	1.70	1.45	1.55	0.80	0.80	0.88	1.02
Ni	Pd	Pt	1.75	1.35	1.44	0.82	0.73	0.77	0.99
Cu	Ag	Au	1.75	1.42	1.42	0.81	0.70	0.67	0.98
Zn	Cd	Hg	1.66	1.46	1.44	0.95	0.85	0.71	1.15

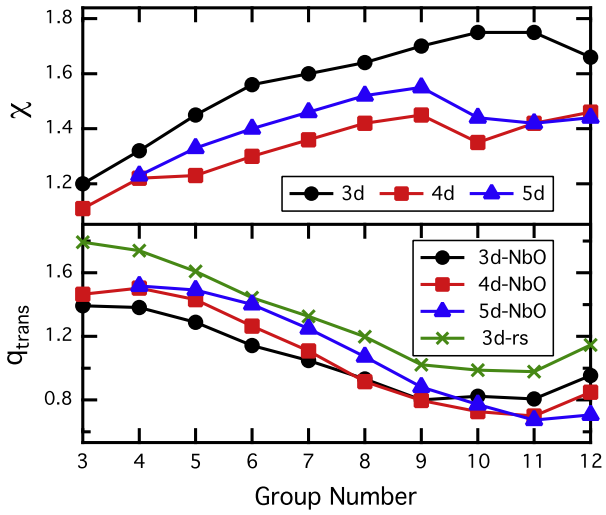

Fig. 9. Electronegativity (χ) of the metals and Bader charge transfer from metal (M) atoms to nitrogen (N) atoms (q_{trans}) of the 3d, 4d and 5d metal, NbO-structured nitrides (MN) versus the group number of their corresponding transition metals. The nitrides corresponding to metals (M) from the 3d, 4d and 5d rows are represented by black circles, red squares and blue triangles respectively. For comparison, 3d metal, rocksalt (rs)-structured nitrides are represented by green ×. For instance, group number 12 stands for Zn (black circle), Cd (red square) and Hg (blue triangle). The data in the two panels suggests anti-correlation of q_{trans} with χ. (For interpretation of the references to color in this figure legend, the reader is referred to the web version of this article.)

transition metals, and a bit unclear for ones with 3d transition metals. This is one of the first systematic investigations of such a large number of compounds showing such a trend. As a specific example, we observe that VN has two to four times larger number of states at E_F than the other three nitrides in Fig. 7. Corresponding with this high number of states is its low hardness seen in Fig. 4.

Table 6 and Fig. 9 show electronegativity (χ) and Bader charge transfer (q_{trans}) of the 29 NbO-structured nitrides. Values of Bader charge transfer for the rs-structured nitrides with 3d transition metals are provided for comparison as well. Values of χ are obtained from the literature [103]. It is clear that the two quantities are directly anti-correlated as expected from their definitions. No correlation of the charge transfer or electronegativity with hardness is evident. We also notice that rs-structured nitrides generally have higher values of q_{trans} than NbO-structured ones with the same metals. Considering rs-structured nitrides have higher values of lattice constant than NbO-structured ones, they would have had lower values of q_{trans}. Therefore, the higher values of q_{trans} for the rs-structured ones may be attributed to a larger coordination number, 6 in its structure, in contrast to 4 in the NbO structure.

4. Conclusion

In this study, we performed *ab initio* calculations on 29 nitride phases of transition metals from the 3d, 4d and 5d rows in NbO structure. We calculated the cohesive energy (E_{coh}) and compared it to that of the corresponding rs-structured nitrides, which have been synthesized or estimated from experimental data. The energetic stability of NbO structure is found to be similar to that of rs structure and in some cases lower than that. We calculated the lattice constant (a) and bulk modulus (B), and observed the anti-correlation between them. We calculated the elastic constants C_{11}, C_{12} and C_{44}, and derived mechanical moduli and ratios with effective medium theory. We observed the correlation between the shear modulus (G), Pugh's ratio (k) and derived Vickers hardness (H_V) with a recently proposed formula. CrN, MoN and WN in NbO structure show values of H_V larger than 20 GPa. We found by comparison with rs structure, that the trends of these mechanical quantities vary greatly for different structures even if the composition stays the same. Within the same structure type, 3d, 4d and 5d metal nitrides behave similarly. We computed Debye temperature and demonstrated its correlation with H_V as proposed by Madelung, Einstein and Deus. The LDOS figures of several nitrides that demonstrate the trends in our systematic study were plotted. We showed systematically that C_{44}, G, k and H_{VT} are anti-correlated with the number of electronic states around E_F, leading to a semi-quantitative link of nitride electronic structure to mechanical instability and hardness. Lastly, Bader charge transfer from metal to nitrogen atom was analyzed throughout the 29 nitrides we studied and comparison with rs structure was provided.

Acknowledgments

The authors thank the Ohio Supercomputer Center (OSC) for the computing resources. We thank the National Science Foundation CMMI 1234777, CNS 0855134, DMR CMMI 0928440 and CMMI 0933069 for funding this work.

References

[1] H. Holleck, J. Vac. Sci. Technol. A 4 (1986) 2661–2669, http://dx.doi.org/10.1116/1.573700.
[2] A. Friedrich, B. Winkler, E.A. Juarez-Arellano, L. Bayarjargal, Materials 4 (2011) 1648–1692, http://dx.doi.org/10.3390/ma4101648.
[3] V.V. Brazhkin, A.G. Lyapin, R.J. Hemley, Philos. Mag. A – Phys. Condens. Matter Struct. Defects Mech. Prop. 82 (2002) 231–253.
[4] D.M. Teter, MRS Bull. 23 (1998) 22–27.
[5] J. Haines, J.M. Leger, G. Bocquillon, Annu. Rev. Mater. Res. 31 (2001) 1–23, http://dx.doi.org/10.1146/annurev.matsci.31.1.1.
[6] J. Musil, Surf. Coat. Technol. 125 (2000) 322–330, http://dx.doi.org/10.1016/s0257-8972(99)00586-1.
[7] X.J. Chen, V.V. Struzhkin, Z.G. Wu, M. Somayazulu, J. Qian, S. Kung, A.N. Christensen, Y.S. Zhao, R.E. Cohen, H.K. Mao, R.J. Hemley, P. Natl, Acad. Sci. USA 102 (2005) 3198–3201, http://dx.doi.org/10.1073/pnas.0500174102.
[8] A. Salamat, A.L. Hector, P. Kroll, P.F. McMillan, Coord. Chem. Rev. 257 (2013) 2063–2072, http://dx.doi.org/10.1016/j.ccr.2013.01.010.
[9] A.Y. Liu, M.L. Cohen, Science 245 (1989) 841–842, http://dx.doi.org/10.1126/science.245.4920.841.
[10] S.H. Jhi, J. Ihm, S.G. Louie, M.L. Cohen, Nature 399 (1999) 132–134, http://dx.doi.org/10.1038/20148.
[11] S.H. Jhi, S.G. Louie, M.L. Cohen, J. Ihm, Phys. Rev. Lett. 86 (2001) 3348–3351, http://dx.doi.org/10.1103/PhysRevLett.86.3348.
[12] S.H. Jhi, S.G. Louie, M.L. Cohen, J.W. Morris, Phys. Rev. Lett. 87 (2001) 075503, http://dx.doi.org/10.1103/PhysRevLett.87.075503.
[13] S. Kodambaka, S.V. Khare, I. Petrov, J.E. Greene, Surf. Sci. Rep. 60 (2006) 55–77, http://dx.doi.org/10.1016/j.surfrep.2005.10.002.
[14] S. Kodambaka, S.V. Khare, V. Petrova, D.D. Johnson, I. Petrov, J.E. Greene, Phys. Rev. B 67 (2003) 035409, http://dx.doi.org/10.1103/PhysRevB.67.035409.
[15] F.M. Gao, J.L. He, E.D. Wu, S.M. Liu, D.L. Yu, D.C. Li, S.Y. Zhang, Y.J. Tian, Phys. Rev. Lett. 91 (2003) 015502, http://dx.doi.org/10.1103/PhysRevLett.91.015502.
[16] F.M. Gao, L.H. Gao, J. Superhard Mater. 32 (2010) 148–166, http://dx.doi.org/10.3103/s1063457610030020.
[17] X.Q. Chen, H.Y. Niu, D.Z. Li, Y.Y. Li, Intermetallics 19 (2011) 1275–1281, http://dx.doi.org/10.1016/J.Intermet.03.026.

[18] Y. Tian, B. Xu, Z. Zhao, Int. J. Refract. Met. Hard Mater. 33 (2012) 93–106, http://dx.doi.org/10.1016/j.ijrmhm.2012.02.021.
[19] G. Travaglini, F. Marabelli, R. Monnier, E. Kaldis, P. Wachter, Phys. Rev. B 34 (1986) 3876–3882, http://dx.doi.org/10.1103/PhysRevB.34.3876.
[20] J.P. Dismukes, W.M. Yim, V.S. Ban, J. Cryst. Growth 13 (1971) 365.
[21] J.P. Dismukes, W.M. Yim, J.J. Tietjen, R.E. Novak, J. Cryst. Growth 9 (1971) 295, http://dx.doi.org/10.1016/0022-0248(71)90244-2.
[22] D. Gall, I. Petrov, N. Hellgren, L. Hultman, J.E. Sundgren, J.E. Greene, J. Appl. Phys. 84 (1998) 6034–6041, http://dx.doi.org/10.1063/1.368913.
[23] D. Gall, I. Petrov, L.D. Madsen, J.E. Sundgren, J.E. Greene, J. Vac. Sci. Technol. A 16 (1998) 2411–2417, http://dx.doi.org/10.1116/1.581360.
[24] T.D. Moustakas, R.J. Molnar, J.P. Dismukes, Proceedings of the First Symposium on III–V Nitride Materials and Processes, vol. 96, 1996, pp. 197–204.
[25] H. Al-Brithen, A.R. Smith, Appl. Phys. Lett. 77 (2000) 2485–2487, http://dx.doi.org/10.1063/1.1318227.
[26] H.A.H. Al-Brithen, E.M. Trifan, D.C. Ingram, A.R. Smith, D. Gall, J. Cryst. Growth 242 (2002) 345–354, http://dx.doi.org/10.1016/s0022-0248(02)01447-1.
[27] A.R. Smith, H.A.H. Al-Brithen, D.C. Ingram, D. Gall, J. Appl. Phys. 90 (2001) 1809–1816, http://dx.doi.org/10.1063/1.1388161.
[28] H.H. Chen, F. Peng, H.K. Mao, G.Y. Shen, H.P. Liermann, Z.O. Li, J.F. Shu, J. Appl. Phys. 107 (2010) 113503, http://dx.doi.org/10.1063/1.3392848.
[29] K. Liu, X.L. Zhou, H.H. Chen, L.Y. Lu, Physica B 407 (2012) 3617–3621, http://dx.doi.org/10.1016/j.physb.2012.05.038.
[30] W.J. Meng, G.L. Eesley, Thin Solid Films 271 (1995) 108–116, http://dx.doi.org/10.1016/0040-6090(95)06875-9.
[31] C.S. Shin, D. Gall, N. Hellgren, J. Patscheider, I. Petrov, J.E. Greene, J. Appl. Phys. 93 (2003) 6025–6028, http://dx.doi.org/10.1063/1.1568521.
[32] O. Shebanova, E. Soignard, P.F. McMillan, High Pressure Res. 26 (2006) 87–97, http://dx.doi.org/10.1080/08957950600765186.
[33] M. Mattesini, R. Ahuja, B. Johansson, Phys. Rev. B 68 (2003) 184108, http://dx.doi.org/10.1103/PhysRevB.68.184108.
[34] A. Zerr, N. Chigarev, R. Brenner, D.A. Dzivenko, V. Gusev, Phys. Status Solidi – R 4 (2010) 353–355, http://dx.doi.org/10.1002/pssr.201004345.
[35] D.A. Dzivenko, A. Zerr, R. Boehler, R. Riedel, Solid State Commun. 139 (2006) 255–258, http://dx.doi.org/10.1016/j.ssc.2006.06.020.
[36] D. Dzivenko, A. Zerr, N. Guignot, M. Mezouar, R. Riedel, Epl 92 (2010) 66001, http://dx.doi.org/10.1209/0295-5075/92/66001.
[37] A. Friedrich, B. Winkler, L. Bayarjargal, E.A.J. Arellano, W. Morgenroth, J. Biehler, F. Schroder, J.Y. Yan, S.M. Clark, J. Alloys Compd. 502 (2010) 5–12, http://dx.doi.org/10.1016/j.jallcom.2010.04.113.
[38] P. Kroll, T. Schroter, M. Peters, Angew. Chem. Int. Ed. 44 (2005) 4249–4254, http://dx.doi.org/10.1002/anie.200462980.
[39] E. Soignard, O. Shebanova, P.F. McMillan, Phys. Rev. B 75 (2007) 014104, http://dx.doi.org/10.1103/PhysRevB.75.014104.
[40] W.W. Lei, D. Liu, X.F. Li, J. Zhang, Q. Zhou, J.Z. Hu, Q.L. Cui, G.T. Zou, J. Phys.-Condens. Matter 9 (2007) 425233, http://dx.doi.org/10.1088/0953-8984/19/42/425233.
[41] A. Zerr, G. Miehe, J.W. Li, D.A. Dzivenko, V.K. Bulatov, H. Hofer, N. Bolfan-Casanova, M. Fialin, G. Brey, T. Watanabe, M. Yoshimura, Adv. Funct. Mater. 19 (2009) 2282–2288, http://dx.doi.org/10.1002/adfm.200801923.
[42] C.S. Shin, Y.W. Kim, D. Gall, J.E. Greene, I. Petrov, Thin Solid Films 402 (2002) 172–182, http://dx.doi.org/10.1016/s0040-6090(01)01618-2.
[43] W.K. Grant, C. Loomis, J.J. Moore, D.L. Olson, B. Mishra, A.J. Perry, Surf. Coat. Technol. 86–7 (1996) 788–796, http://dx.doi.org/10.1016/s0257-8972(96)03071-x.
[44] P. Hones, N. Martin, M. Regula, F. Levy, J. Phys. D – Appl. Phys. 36 (2003) 1023–1029, http://dx.doi.org/10.1088/0022-3727/36/8/313.
[45] F. Rivadulla, M. Banobre-Lopez, C.X. Quintela, A. Pineiro, V. Pardo, D. Baldomir, M.A. Lopez-Quintela, J. Rivas, C.A. Ramos, H. Salva, J.S. Zhou, J.B. Goodenough, Nat. Mater. 8 (2009) 947–951, http://dx.doi.org/10.1038/nmat2549.
[46] X.Y. Zhang, J.S. Chawla, R.P. Deng, D. Gall, Phys. Rev. B 84 (2011) 073101, http://dx.doi.org/10.1103/PhysRevB.84.073101.
[47] M. Urgen, O.L. Eryilmaz, A.F. Cakir, E.S. Kayali, B. Nilufer, Y. Isik, Surf. Coat. Technol. 94–5 (1997) 501–506, http://dx.doi.org/10.1016/s0257-8972(97)00432-5.
[48] D. Machon, D. Daisenberger, E. Soignard, G. Shen, T. Kawashima, E. Takayama-Muromachi, P.F. McMillan, Phys. Status Solidi A 203 (2006) 831–836, http://dx.doi.org/10.1002/pssa.200521008.
[49] E. Soignard, P.F. McMillan, T.D. Chaplin, S.M. Farag, C.L. Bull, M.S. Somayazulu, K. Leinenweber, Phys. Rev. B 68 (2003) 132101, http://dx.doi.org/10.1103/PhysRevB.68.132101.
[50] Y. Ma, Q. Cui, L. Shen, Z. He, J. Appl. Phys. 102 (2007) 013525, http://dx.doi.org/10.1063/1.2751087.
[51] A. Friedrich, B. Winkler, L. Bayarjargal, W. Morgenroth, E.A. Juarez-Arellano, V. Milman, K. Refson, M. Kunz, K. Chen, Phys. Rev. Lett. 105 (2010) 085504, http://dx.doi.org/10.1103/PhysRevLett. 105.085504.
[52] A. Friedrich, B. Winkler, K. Refson, V. Milman, Phys. Rev. B 82 (2010) 224106, http://dx.doi.org/10.1103/PhysRevB.82.224106.
[53] J.F. Adler, Q. Williams, Earth 110 (2005) B01203, http://dx.doi.org/10.1029/2004jb003103.
[54] A.F. Young, C. Sanloup, E. Gregoryanz, S. Scandolo, R.J. Hemley, H.K. Mao, Phys. Rev. Lett. 96 (2006) 155501, http://dx.doi.org/10.1103/PhysRevLett.96.155501.
[55] J.A. Montoya, A.D. Hernandez, C. Sanloup, E. Gregoryanz, S. Scandolo, Appl. Phys. Lett. 90 (2007) 011909, http://dx.doi.org/10.1063/1.2430631.
[56] J.C. Crowhurst, A.F. Goncharov, B. Sadigh, C.L. Evans, P.G. Morrall, J.L. Ferreira, A.J. Nelson, Science 311 (2006) 1275–1278, http://dx.doi.org/10.1126/science.1121813.
[57] J.C. Crowhurst, A.F. Goncharov, B. Sadigh, J.M. Zaug, D. Aberg, Y. Meng, V.B. Prakapenka, J. Mater. Res. 23 (2008) 1–5, http://dx.doi.org/10.1557/jmr.2008.0027.
[58] D. Aberg, P. Erhart, J. Crowhurst, J.M. Zaug, A.F. Goncharov, B. Sadigh, Phys. Rev. B 82 (2010) 104116, http://dx.doi.org/10.1103/PhysRevB.82.104116.
[59] E. Gregoryanz, C. Sanloup, M. Somayazulu, J. Badro, G. Fiquet, H.K. Mao, R.J. Hemley, Nat. Mater. 3 (2004) 294–297, http://dx.doi.org/10.1038/nmat1115.
[60] J.G. Zhao, S.J. You, L.X. Yang, C.Q. Jin, Solid State Commun. 150 (2010) 1521–1524, http://dx.doi.org/10.1016/j.ssc.2010.06.012.
[61] Y.V. Butenko, L. Alves, A.C. Brieva, J. Yang, S. Krishnamurthy, L. Siller, Chem. Phys. Lett. 430 (2006) 89–92, http://dx.doi.org/10.1016/j.cplett.2006.08.096.
[62] L. Siller, M.R.C. Hunt, J.W. Brown, J.M. Coquel, P. Rudolf, Surf. Sci. 513 (2002) 78–82, http://dx.doi.org/10.1016/s0039-6028(02)01150-0.
[63] L. Siller, N. Peltekis, S. Krishnamurthy, Y. Chao, S.J. Bull, M.R.C. Hunt, Appl. Phys. Lett. 86 (2005) 221912, http://dx.doi.org/10.1063/1.1941471.
[64] S. Krishnamurthy, M. Montalti, M.G. Wardle, M.J. Shaw, P.R. Briddon, K. Svensson, M.R.C. Hunt, L. Siller, Phys. Rev. B 70 (2004) 045414, http://dx.doi.org/10.1103/PhysRevB.70.045414.
[65] J.G. Zhao, L.X. Yang, S.J. You, F.Y. Li, C.Q. Jin, J. Liu, Physica B 405 (2010) 1836–1838, http://dx.doi.org/10.1016/j.physb.2010.01.057.
[66] S.K.R. Patil, S.V. Khare, B.R. Tuttle, J.K. Bording, S. Kodambaka, Phys. Rev. B 73 (2006) 104118, http://dx.doi.org/10.1103/PhysRevB.73.104118.
[67] Z.T.Y. Liu, X. Zhou, S.V. Khare, D. Gall, J. Phys.-Condens. Matter 26 (2014) 025404, http://dx.doi.org/10.1088/0953-8984/26/2/025404.
[68] E.J. Zhao, J.P. Wang, J. Meng, Z.J. Wu, Comput. Mater. Sci. 47 (2010) 1064–1071, http://dx.doi.org/10.1016/j.commatsci.2009.12.011.
[69] E.J. Zhao, Z.J. Wu, J. Solid State Chem. 181 (2008) 2814–2827, http://dx.doi.org/10.1016/j.jssc.2008.07.022.
[70] S.K.R. Patil, N.S. Mangale, S.V. Khare, S. Marsillac, Thin Solid Films 517 (2008) 824–827, http://dx.doi.org/10.1016/j.tsf.2008.07.034.
[71] W. Chen, J.Z. Jiang, J. Alloys Compd. 499 (2010) 243–254, http://dx.doi.org/10.1016/j.jallcom.2010.03.176.
[72] Y.C. Wang, T.K. Yao, H. Li, J. Lian, J.H. Li, Z.P. Li, J.W. Zhang, H.Y. Gou, Comput. Mater. Sci. 56 (2012) 116–121, http://dx.doi.org/10.1016/j.commatsci.2012.01.005.
[73] W. Kohn, L.J. Sham, Phys. Rev. 140 (1965) 1133.
[74] G. Kresse, J. Hafner, Phys. Rev. B 48 (1993) 13115–13118, http://dx.doi.org/10.1103/PhysRevB.48.13115.
[75] G. Kresse, J. Furthmuller, Phys. Rev. B 54 (1996) 11169–11186, http://dx.doi.org/10.1103/PhysRevB.54.11169.
[76] G. Kresse, J. Furthmuller, Comput. Mater. Sci. 6 (1996) 15–50, http://dx.doi.org/10.1016/0927-0256(96)00008-0.
[77] D. Vanderbilt, Phys. Rev. B 41 (1990) 7892–7895, http://dx.doi.org/10.1103/PhysRevB.41.7892.
[78] G. Kresse, J. Hafner, J. Phys.-Condens. Matter 6 (1994) 8245–8257, http://dx.doi.org/10.1088/0953-8984/6/40/015.
[79] D.M. Ceperley, B.J. Alder, Phys. Rev. Lett. 45 (1980) 566–569, http://dx.doi.org/10.1103/PhysRevLett.45.566.
[80] J.P. Perdew, J.A. Chevary, S.H. Vosko, K.A. Jackson, M.R. Pederson, D.J. Singh, C. Fiolhais, Phys. Rev. B 46 (1992) 6671–6687, http://dx.doi.org/10.1103/PhysRevB.46.6671.
[81] C. Stampfl, W. Mannstadt, R. Asahi, A.J. Freeman, Phys. Rev. B 63 (2001) 155106, http://dx.doi.org/10.1103/PhysRevB.63.155106.
[82] Y.M. Juan, E. Kaxiras, Phys. Rev. B 48 (1993) 14944–14952, http://dx.doi.org/10.1103/PhysRevB.48.14944.
[83] H.J. Monkhorst, J.D. Pack, Phys. Rev. B 13 (1976) 5188–5192, http://dx.doi.org/10.1103/PhysRevB.13.5188.
[84] J.D. Pack, H.J. Monkhorst, Phys. Rev. B 16 (1977) 1748–1749, http://dx.doi.org/10.1103/PhysRevB.16.1748.
[85] F.D. Murnaghan, P. Natl, Acad. Sci. USA 30 (1944) 244–247, http://dx.doi.org/10.1073/pnas.30.9.244.
[86] H.Z. Fu, D.H. Li, F. Peng, T. Gao, X.L. Cheng, Comput. Mater. Sci. 44 (2008) 774–778, http://dx.doi.org/10.1016/J.Commatsci.05.026.
[87] M. Mehl, J. Osburn, D. Papaconstantopoulos, B. Klein, Phys. Rev. B 41 (1990) 10311–10323, http://dx.doi.org/10.1103/PhysRevB.41.10311.
[88] M. Mehl, J. Osburn, D. Papaconstantopoulos, B. Klein, Phys. Rev. B 42 (1990) 5362–5363, http://dx.doi.org/10.1103/PhysRevB.42.5362.
[89] S.C. Abrahams, F.S.L. Hsu, J. Chem. Phys. 63 (1975) 1162–1165, http://dx.doi.org/10.1063/1.431443.
[90] E. Madelung, Phys. Z 11 (1910) 898.
[91] A. Einstein, Ann. Phys. (Leipz.) 34 (1911) 590.
[92] A. Einstein, Ann. Phys. (Leipz.) 35 (1911) 679.
[93] P. Deus, H.A. Schneider, Cryst. Res. Technol. 18 (1983) 491–500, http://dx.doi.org/10.1002/crat.2170180410.
[94] P.E. Blöchl, O. Jepsen, O.K. Andersen, Phys. Rev. B 49 (1994) 16223–16233, http://dx.doi.org/10.1103/PhysRevB.49.16223.
[95] A. Arnaldsen, W. Tang, S. Chill, G. Henkelman, Bader Charge Analysis. <http://theory.cm.utexas.edu/bader/> (access 17.11.13).

[96] G. Henkelman, A. Arnaldsson, H. Jonsson, Comput. Mater. Sci. 36 (2006) 354–360, http://dx.doi.org/10.1016/j.commatsci.2005.04.010.
[97] E. Sanville, S.D. Kenny, R. Smith, G. Henkelman, J. Comput. Chem. 28 (2007) 899–908, http://dx.doi.org/10.1002/jcc.20575.
[98] W. Tang, E. Sanville, G. Henkelman, J. Phys.-Condens. Matter 21 (2009) 084204, http://dx.doi.org/10.1088/0953-8984/21/8/084204.
[99] R.F.W. Bader, Atoms in Molecules: A Quantum Theory, Oxford University Press, New York, 1990.
[100] F.W. Bieglerkonig, R.F.W. Bader, T.H. Tang, J. Comput. Chem. 3 (1982) 317–328, http://dx.doi.org/10.1002/jcc.540030306.
[101] The PAW and US-PP Database. <http://cms.mpi.univie.ac.at/vasp-workshop/slides/pseudoppdatabase.pdf> (access 17.11.13).
[102] J. Häglund, G. Grimvall, T. Jarlborg, A.F. Guillermet, Phys. Rev. B 43 (1991) 14400–14408, http://dx.doi.org/10.1103/PhysRevB.43.14400.
[103] A.L. Allred, E.G. Rochow, J. Inorg. Nucl. Chem. 5 (1958) 264–268.